WM2018 Conference, March 18 - 22, 2018, Phoenix, Arizona, USA

The DISTINCTIVE University Consortium: Structural Integrity - 18272

*R.J. Lunn[a], A. Hamilton[a], M. Pedrotti[a], P. Bots[a], C. Wong[a], G. El Mountassir[a], J. Renshaw[a], R. Maddelena[a], C. Zhao[b], L. Sun[b], R Stolkin[b], M. Fairweather[c], L. Tovey[c], C. Boxall[d], J.A. Hriljac[e], N.C. Hyatt[f], N. Kaltsoyannis[g], W.E. Lee[h], D. Read[i], T.B. Scott[i]

[a]Dept. of Civil & Environmental Engineering, University of Strathclyde, Glasgow G1 1XQ, UK
[b]School of Metallurgy and Materials, University of Birmingham, Birmingham, B15 2TT, UK
[c]School of Chemical & Process Engineering, University of Leeds, Leeds LS2 9JT, UK
[d]Dept. of Engineering, Lancaster University, Lancaster LA1 4YR, UK
[e]School of Chemistry, University of Birmingham, Birmingham B15 2TT, UK
[f]Dept. of Materials Science & Engineering, University of Sheffield, Sheffield S1 3JD, UK
[g]School of Chemistry, University of Manchester, Manchester M13 9PL, UK
[h]Dept. of Materials, Imperial College London, London SW7 2AZ, UK
[i]Department of Chemistry, University of Surrey, Guildford GU2 7XH, UK
[j]School of Physics, University of Bristol, Bristol BS8 1TL, UK

ABSTRACT

The Engineering and Physical Sciences Research Council (EPSRC) sponsored DISTINCTIVE consortium (Decommissioning, Immobilisation and Storage Solutions for Nuclear Waste Inventories) is developing technologies for civil infrastructure repair, in-situ subsurface waste immobilisation, and groundwater protection during construction and decommissioning. The consortium has contributed to the development of skilled cross-disciplinary civil engineers and scientists, that have the knowledge and experience required to develop engineering solutions tailored for application within radiologically contaminated sites. The Structural Integrity Theme focuses on challenges ranging from site-scale infrastructure preservation and restoration, through injectable ground barriers for risk mitigation, to the remote characterisation and handling of individual waste packages. The main aim of the theme is to develop novel engineering solutions, tailored for use on radiologically contaminated sites, for: ground protection; infrastructure characterisation; concrete restoration and waste characterisation. Technologies should minimise current, and future, radiation exposure of the workforce whilst providing economically viable engineering solutions.

INTRODUCTION

Nuclear power stations contain huge volumes of mainly concrete assets, both above and below ground. Many sites have a history of plant-life extensions, multiple phases of construction and changing operational requirements that have resulted in complex overcrowded site layouts with ageing structures that contain hazardous materials. Further, many of these structural assets have withstood harsh environmental conditions (freeze-thaw, high salinity, fluctuating moisture contents) for time-scales well over their design lives. These complex structural assets must be monitored, repaired where necessary, and ultimately, decommissioned. Critical to their future management is limiting worker radiation exposure, protecting the environment and minimising the volume of radiologically contaminated waste for disposal.

The EPSRC sponsored DISTINCTIVE consortium (Decommissioning, Immobilisation and Storage Solutions for Nuclear Waste Inventories), under its Structural Integrity Theme focuses on challenges ranging from site-scale infrastructure preservation and restoration, through injectable ground barriers for risk mitigation, to the remote characterisation and handling of individual waste packages.

The main aim of the theme is to develop novel engineering solutions, tailored for use on radiologically contaminated sites, for: ground protection; infrastructure characterisation; concrete restoration and waste

* *Corresponding author, e-mail: Rebecca.lunn@strath.ac.uk*

characterisation. Technologies should minimise current, and future, radiation exposure of the workforce whilst providing economically viable engineering solutions. The objectives are:

- To develop in-situ ground barriers that could act as a 'second skin' surrounding on-site structures, such as silos and ponds, for prevention of subsurface radionuclide migration.
- To develop smart solutions for remote crack detection, civil infrastructure health prediction and building preservation that can be retrofitted to existing sites.
- To develop autonomous systems with increased functionality and to coordinate them through a Computer Aided Design (CAD)-based real-time management system, to facilitate planning and execution of decommissioning works.

These objectives are being met by several linked projects in three work packages, the details of which are given in Table I.

TABLE I. Projects, researcher type and university undertaking work in the structural integrity theme, organised by work package ([a]indicates an associated PhD or Post Doctoral Research Associate, PDRA, that is not directly funded by the DISTINCTIVE project).

Project Title	**Type**	**University**
Physical Ground Barriers for In-Situ Contaminant Containment		
In-situ ground contaminant containment (physical barrier)	PDRA	Strathclyde
Immobilisation and containment of radioactive waste using colloidal silica-based grout	PDRA[a]	Strathclyde
In-situ ground contaminant containment (physical barrier)	PhD	Strathclyde
Development of novel, low cost biomineral permeable reactive barriers for radionuclide remediation	PhD[a]	Strathclyde
Remote Crack Detection, Infrastructure Health Prediction and Building Preservation		
Nano-cracking of cement phases: reactivity and dissolution	PhD	Strathclyde
Consolidation in cement and concrete	PhD	Strathclyde
Monitoring of moisture and chloride in contaminated storage structures	PhD	Strathclyde
Simulating radiation damage in cement	PhD[a]	Queen's Univ. Belfast
Impact of recycled concrete fines on the engineering performance of cementitious infill	PhD[a]	Leeds
Integrated sensors for infrastructure	PhD[a]	Strathclyde
Development and Real-time Management of Autonomous Systems for Decommissioning		
Production of real-time segmented as-built CAD models for the planning and execution of remote and human intervention tasks	PhD	Birmingham

This paper presents highlights of research from each of the three areas: (1) In-situ barriers for groundwater protection, (2) Consolidation in cement and concrete, and (3) Real-time management of autonomous systems for decommissioning.

IN-SITU BARRIERS FOR GROUNDWATER PROTECTION

The long and varied UK history of nuclear reactor research, nuclear power production, fuel reprocessing and storage of radioactive wastes has resulted in a legacy of ageing structures, multiple waste streams and structurally complex sites. On such sites, soils may be radiologically contaminated and some containment structures may be in poor condition. To reduce hazard, programmes of waste retrieval, processing and storage are underway. During waste retrieval and decommissioning operations, structures (and their surrounding soils) are subject to changes in loading conditions, resulting in an increased risk of radionuclide releases into the subsurface environment. This risk could be mitigated by the prior formation of ground barriers. Near-surface ground barriers are traditionally formed via excavation and emplacement of bentonite-slurry trenches, since the high viscosity of cements prevents their injection at shallow depths (<20m below surface). Excavation of soils on radiologically-contaminated sites, however, presents a significant hazard to workers and is not desirable. A viable alternative could be colloidal silica, which can be injected at low pressure into near-surface soils, and then 'gelled' to form low permeability, in-situ hydraulic barriers for ground protection.

Colloidal silica has been successfully adopted as a fluid-flow control system within the petroleum industry since the late 1980s [1]. Consolidated core plugs of fully cured colloidal silica were observed to withstand applied pressure gradients of more than (56 MPa/m) before exhibiting any permeability change. Passive site remediation proposed by Gallagher [2] studied the application of colloidal silica as a non-disruptive mitigation technique to sites susceptible to liquefaction. Desirable characteristics were long injection periods up to 100 days for low concentration solutions of approximately 10 to 20% colloidal silica concentration. Du Pont Chemicals R & D initiated work examining the feasibility of colloidal silica grout as a soil remediation technique through a series of bench-scale laboratory studies. Gelled colloidal silica was seen to prevent leaching of fluids containing metals through permeability reduction. Further, high affinities for the adsorption of metals from solution were seen by the colloidal silica gel itself [3]. Similarly, the stabilization process of chromium contaminated soils using colloidal silica was investigated by Yossapol and Meegoda [4].

In the 90s, Lawrence Berkley National Laboratory and Brookhaven National Laboratory carried out in-situ [5-9] and laboratory [10-12] tests to demonstrate the use of silica colloids for permeation grouting for containment technology. For the construction and operation of a nuclear waste repository in hard rock, researchers at Chalmers University of Technology investigated the application of colloidal silica grout to minimise water ingress in shafts and tunnels. In order to evaluate penetrability, laboratory mechanical tests on colloidal silica [13, 14] and field tests [15, 16] were performed. More recently, colloidal silica has been adopted in the tunnelling and underground construction industry for preventing water ingress as a secondary injection grout during the pre-injection stage (i.e. injecting in advance of the tunnel face during excavation) (e.g. Butrón, Gustafson [17], Bahadur, Holter [18]).

Despite the documented success of colloidal silica based grouts, research has not translated into widespread industrial use. Yet colloidal silica has the potential to transform the environmental hazard associated with dismantling and decommissioning by pre-treating the ground surrounding, and beneath, nuclear structures. Key factors in the limited commercial uptake have been: the lack of a predictive model for colloidal silica grout gelling in natural environments, that would allow engineers to predict grout penetration distances; the lack of mechanical data on the properties of the grouted soil; the need to investigate grout-radionuclide interactions for contaminated soils.

Modeling Colloidal Silica Penetration

The potential of colloidal silica as a favorable grouting material exists due to: i) its initial low viscosity (close to water), ii) its low hydraulic conductivity after gelling (of the order of 10^{-7} cm/s), iii) the very low injection pressures required, iv) its controllable set/gel times (from minutes to several days), v) the fact it is environmentally inert and vi) its small particle size (less than hundreds of nanometres).

Colloidal silica is a stable aqueous suspension of microscopic silica particles (SiO_2). In alkaline solutions and low electrolyte concentration colloidal silica is stable. Destabilization of the solution and subsequent gelation can be induced by destabilization of the particle repulsive forces through the addition of an accelerator electrolyte compound. This process, shown in Fig. 1a results in a rapid viscosity increase after a given period of time (gel time). Gel time has been proven to depend on colloidal particle size, colloidal particle concentration, electrolyte concentration, cation valence, cation atomic mass and temperature (not considered here) [19].

Pedrotti et al. [19] describes an electrochemically inferred analytical model of grout gelling . The model is able to predict, for the first time, the grout gelation time and the change in viscosity over time as a function of pH, electrolyte, silica particle size and silica concentration. This model is fundamental to the accurate simulation of grout penetration in a natural environment. Fig.1b shows an example of the model gel time results, versus the experimental data, for variations in solution pH and accelerator concentration. In Figure 2c the change in viscosity over time is plotted for a single accelerator concentration of 2 M for four different values of pH, ranging from 4 to 9. In all experiments, the model provides a good prediction of the experimental observations.

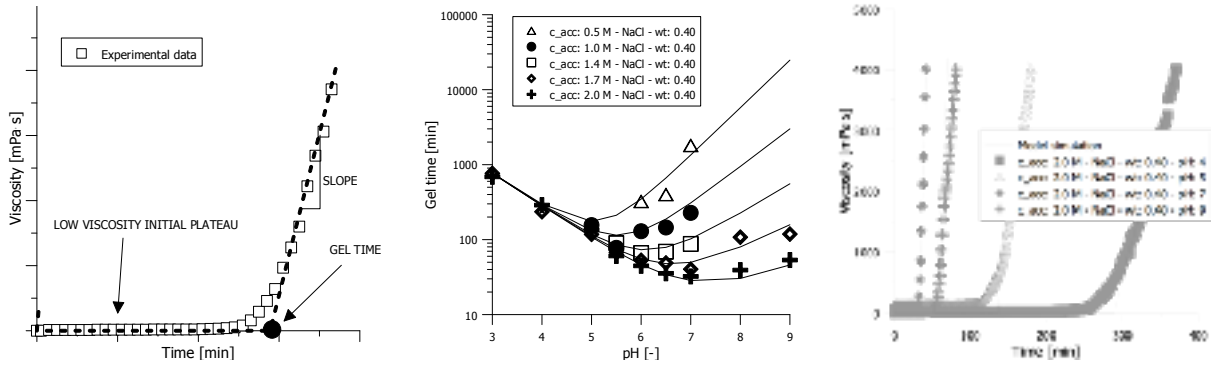

Figure 1. a) Gel time, b) gel time prediction [19], Viscosity prediction ([19])

A key advantage of the model is its ability to simultaneously account for the presence of many different cation species in the estimation of grout gel time and viscosity. This capability provides a useful tool for the design of grout mixes using colloidal silica, that can take account of the situ groundwater composition, overcoming one of the main challenges to grout use within industry.

The analytical model of colloidal silica gelling has since been implemented within a numerical model of grout penetration in a saturated porous media, within the generic finite element software, COMSOL Multiphysics ®. The numerical model implements the generalised form of Darcy's equation for the velocity profile of the injected fluid.

This equation is coupled with a transport model that simulates the transport of two different chemical components: First, the concentration of colloidal silica and second, the concentration of the accelerant. At each time-step and for any given spatial point, the numerical model computes the viscosity of the colloidal silica using the analytical model described above.

To validate the numerical model of grout penetration (i.e. injection and then subsequent gelling) an experimental injection tank (1.3 m x 0.4 m x 0.1 m) was constructed (Figure 2). The tank was filled with 72 kg Leighton Buzzard sand with a median grain diameter d_{50} of 1.2 mm, specific gravity of 2.65 and coefficient of conformity of 1.26, resulting in an average porosity of approximately 0.36. The tank was filled with 17 litres of water and a layer of clay was placed on top of the sand in order to ensure horizontal flow paths (Fig. 2).

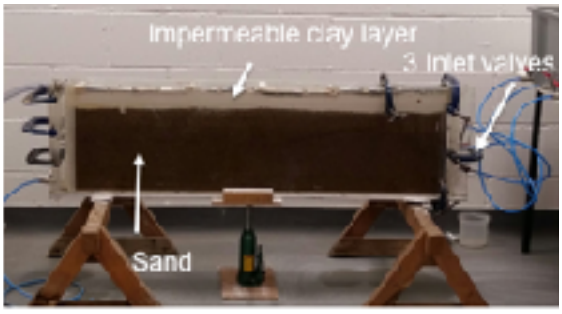

Figure 2. Experimental tank setup

Injection into the tank was performed via three lateral valves connected to a constant-head reservoir on the right-hand side (Fig. 2). Outflow was via a single port connected to a constant head reservoir on the left-hand side.

Preliminary injection of water containing fluorescein was conducted to calibrate the model parameters for flow and transport. Fig. 3 shows the experiment and accompanying numerical simulation for the fluorescein injection after 17 minutes. The experiment and the numerical model are in good agreement, giving calibrated values for hydraulic permittivity and diffusion of $1.89 \cdot 10^{-9}$ m^2 and 0.01 m^2/s respectively.

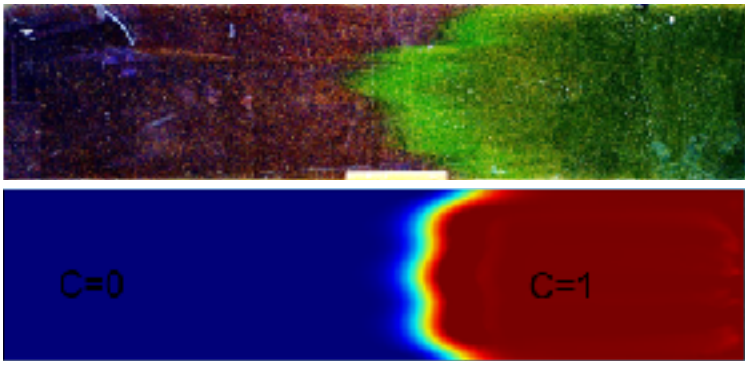

Figure 3. Fluorescein injection. Experiment and simulation comparison

Colloidal silica grout was injected into the tank using an accelerant concentration in the inflow of 1.7 M of NaCl, to produce a predicted grout gel time of 51 minutes. After the grout had gelled, the remaining loose sand in the tank was excavated by hand.
Fig. 4a shows the shape of the grouted sand volume post injection n and subsequent excavation. As expected, the shape of the grout front differs significantly to that of the conservative tracer in Figure 3; due to the density difference between the water and the grout, during injection the denser grout sinks due to gravity. Fig. 4b shows the corresponding model prediction: an accurate injection distance of the grout was predicted. The final shape of the grouted sand differs slightly from the experimental one. This effect is probably due to the slightly increased diffusion coefficient that was used in the numerical model, in order to remove numerical instability issues.

Further tank experiments have been performed varying the soil composition, by introducing a clay lens, and with the addition of saline in-situ groundwater. All model simulations are a good match to the experiments, thus verifying our predictive modelling capability.

a)

b)

Figure 4. Grouted sand after colloidal silica injection. a) experimental grouted sand volume, b) finite element model prediction.

The Mechanical Behavior of Grouted Soils

The mechanical behavior of colloidal silica was investigated in Wong et al. [20]. The aim was to evaluate the drained stress-strain behavior (1-D compression and shear resistance) of colloidal silica-soil systems and to determine the particle interactions between soil and colloidal silica at a micron-scale, so as to provide an understanding of the macroscopic mechanical behavior. A comparison of the shear behavior of sand and colloidal-silica grouted sand, for two different curing times, is shown in Figure 5. The colloidal silica-grouted sand shows an increase in the peak shear strength, when compared to sand only, and odometer tests also showed an increase in the stiffness.

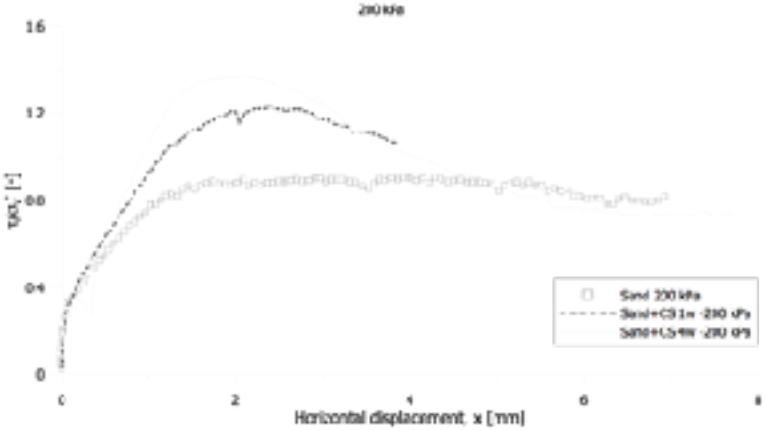

Figure 5. Shear test comparison between grouted sand and sand only.

The hydraulic conductivity of the grouted sand is extremely low, ~10^{-10} m/s, typical of an intact clay. Similar experiments with clay-colloidal silica mixtures showed reduced volumetric deformation, increased stiffness for low values of stress (~100 kPa), and increases in both the peak and the ultimate shear strength. Fig. 6 shows an X-ray computed tomography (X-CT) image of a sample of sand grouted with colloidal silica. Colloidal silica fills most of the voids present between the sand particles (shown by the dark grey in Fig. 6). Air voids would appear black on the image. The whole porosity of the sample now depends only (excluding a few remaining bubbles of air) on the porosity of the colloidal silica matrix. The colloidal silica matrix itself is not visible as the pore size is at least 2-3 orders of magnitude smaller than the maximum resolution of the scanner (~5 microns for beam settings used). It is evident that no pores remain in the grouted sand sample that are due to the original sand structure.

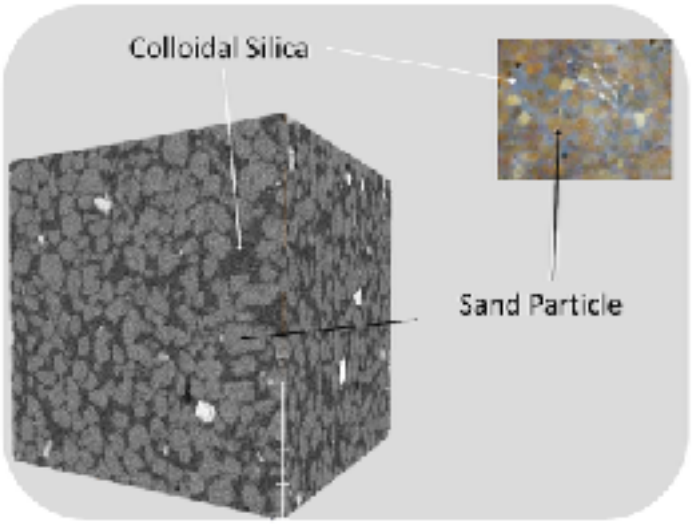

Figure 6. X-CT image of sand grouted with colloidal silica

Grout-Radionuclide Interaction

To test the grout-radionuclide interaction we performed a set of four batch experiments on the desorption of stable isotopes of Sr and Cs adsorbed onto simulated soil materials at pH 7 (714±18 ppm Cs and 1051±25 ppm Sr). The composition of the simulated soil is: 45% quartz, 25% kaolinite, 25% ordered mixed layered illite-smectite (special source clay; CMS: ISCz-1), 3% goethite (FeOOH) and 2% anatase (TiO_2). Two desorption experiments were performed on unconsolidated samples at 0.8g of the simulated soil material in 40ml of either 0 or 10 mM NaCl, to determine the effects of the salinity on the desorption of Sr and Cs. Additionally, two experiments were performed on the desorption of Sr and Cs from 0.8g of the simulated soil material embedded in 6ml of colloidal silica grout with 20ml of 10 mM NaCl. Two simulated soil samples were embedded in colloidal silica grout, with either 1.4 M NaCl or 0.2 M $CaCl_2$ in the accelerant mixed at a ratio of 5 parts colloidal silica to one part accelerant. The pH was measured and solution samples were collected after 10 min, 1 h, 3 h, 5 h, 1 day and 1 week and analysed for Sr and Cs using ion chromatography (Metrohm Professional 850).

The results of the desorption experiments are shown in Figure 7. These preliminary results highlight a couple of differences in the desorption mechanism: (1) the increase in the Sr and Cs concentrations in solution is retarded in the experiments with grouted simulated soil samples; (2) the absolute concentrations released from the grouted simulated soil samples is significantly less compared to the ungrouted simulated soil samples; and (3) the pH during the desorption experiments reach ~7 and ~9.5 in

the supernatant of the ungrouted and grouted soil samples, respectively. To quantify and separate the influences of the pH, the elevated Na^+ or Ca^{2+} concentrations resulting from the accelerant and the diffusion limited mobility (rather than through groundwater flow) of radionuclides within the colloidal silica grout and the subsequent release of these radionuclides into the groundwater experiments are ongoing.

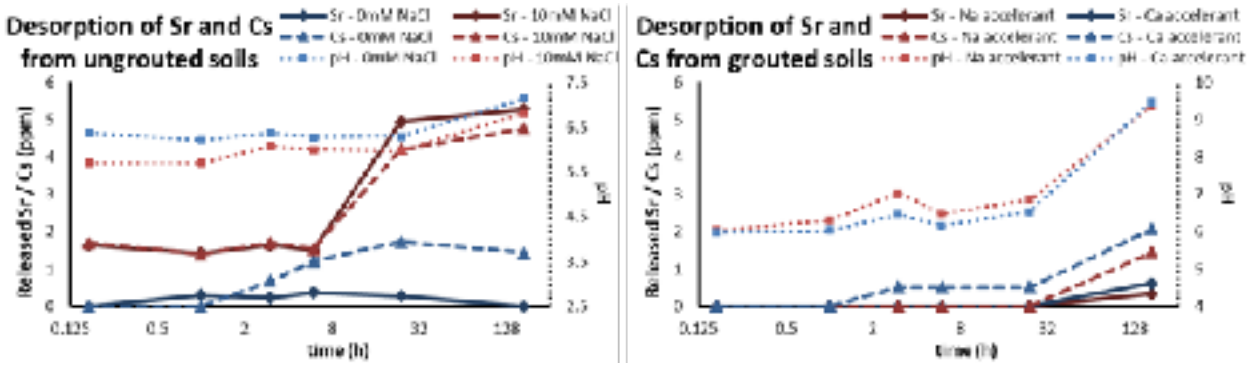

Figure 7 Sr and Cs concentrations and the pH (pH scale is different in both graphs) in the supernatant during the preliminary desorption experiments from unconsolidated simulated soil (ungrouted) and from simulated soil embedded within colloidal silica grout using 1.4 M NaCl or 0.2 M $CaCl_2$ in the accelerant (error on the Sr and Cs concentrations is approximately 0.5ppm and the error on the pH is estimated at 0.02)

CONSOLIDATION OF CEMENT AND CONCRETE

Nuclear sites contain very substantial quantities of cement, much of which is well beyond its design life. The earliest nuclear assets at the Sellafield site date from the 1940s and, hence, are approaching 80 years old. Many ageing structures suffer from crack formation, water penetration and damage mechanisms such as alkali-silica reaction. Thus material properties governing water transport, such as porosity, permeability and strength are altered during ageing.

Portland cement is made up of alite (Ca_3SiO_5), belite Ca_2SiO_4, tricalcium aluminate ($Ca_3Al_2O_6$), and ferrite ($Ca_2(Al_xFe_{2-x})O_5$) plus some gypsum ($Ca(SO_4)\cdot 2H_2O$) and limestone powder. Hydrated Portland cement contains two main mineral phases: $Ca(OH)_2$ (portlandite) and calcium silicate hydrate (C-S-H), the former has a well-defined crystal structure and the latter is poorly crystalline [21]. C-S-H makes up ~ 75 wt% of the final hardened product [22], is responsible for strength development, has a variable stoichiometry and the ability to adsorb contaminants and radionuclides, such as Cs, Zn, Sr, Co, U etc [23, 24]. The production of more C-S-H through the addition of pozzolanic materials gives improved mechanical performance [25] and potentially increased adsorption of radionuclides. Nano-silica addition to cement paste has been shown to increase C-S-H formation and accelerate hydration of any unreacted alite (C_3S), due to the high reactivity of small particles [26]. Research under the structural integrity theme, reported in full in Maddalena and Hamilton (2017) [27], shows how nano-silica, injected into hardened cement paste, reacts with Portlandite already present into the system to produce new C-S-H. This reduces porosity and is a potential technique for protecting cement structures from further degradation.

TABLE II: Characteristics of nano-silica (NS) and silica fume (SF).

Components	NS	SF
State	Aqueous suspension	particles
Chemical composition (>0.2%)		
SiO_2	50%	99.9%

Water	50%	-
Particle size range (nm)	5-20	150-1000
Density (g/cm^3)	1.4	1.6
Specific area (m^2/g)	110-160	15-30

The experiments were carried out on pure hardened cement paste made with CEM II/A-L class 42.5 N bought from Lagan Cement Ltd and deionized water. Nano-silica (NS) suspension LUDOX T-50 and silica fume (SF) ELKEM microsilica were used (TABLE II).

Cement samples were prepared by mixing Portland cement and deionized water at a water to cement (w/c) ratio of 0.4:1 by mixing in a rotary mixer according to BS EN 196-1:2005. Cement paste was cast into plastic moulds (35mm ∅ and 4mm thickness, disc-shaped) and cured under controlled conditions (relative humidity: 98 ± 2% and temperature: 21 ± 2 °C). After 28 days, cement discs were oven-dried at 60 °C for ca. 100 hours, until the change in mass was negligible. Whilst oven drying is known to affect the pore-structure of cement, the aim here was to measure mass gain rather than micro-structural characterization.

Experimental Setup for Cement Consolidation

Nano-silica injection was carried out by varying three parameters: injection period, percentage of nano-silica injected and silica particle size with a constant applied pressure head. Silica solutions were prepared using nano-silica stock suspension or solid silica fume, mixed with deionized water. In order to investigate how the penetration depth in the disc varies with nano-silica content, three different percentages (10, 15 and 20 wt. %) were used, for a total injection time of 14 days. The effect of injection time was determined by keeping cement discs under injection for 7, 14 and 28 days with 10 wt.% nano-silica content. To compare the reactivity and effect of particle size on penetration depth, new samples were injected with a 10% or 20% solution of silica fume for a period of 14 days.

The cement disc was fixed in place at the bottom of a PVC pipe of 2 m length and 40 mm internal diameter. The pipe was clamped vertically in place. A solution of nano-silica or silica fume of known concentration was slowly poured into the pipe from the top, in order to minimize the density gradient. The length of pipe used gives a constant hydrostatic pressure of 20 kPa at the bottom of the pipe, where the OPC specimen is placed. After filling the pipe, a plastic cap was placed at the top of the pipe to avoid evaporation of the solution. At the end of the injection period, the disc was removed and oven-dried at 60 °C for ca. 100 hours. The sample mass was recorded before and after injection to quantify the amount of silica in the pores. Open porosity (φ) was determined by measuring the total water amount in each sample after oven-drying at 60 °C followed by overnight saturation in a vacuum chamber.

The ability of injected silica to react with calcium hydroxide (CH) present in the hydrated cement paste to form additional calcium silicate hydrates (C-S-H) was determined by the quantity of calcium hydroxide and C-S-H in the treated hydrated cement paste compared with the control sample by thermogravimetric analysis (TGA). Mineralogical composition of silica injected specimens was analyzed using powder X-ray diffraction (XRD).

Cement Consolidation Results and Discussion

Mass measurements showed that after 14 days of nano-silica injection, the mass increase is directly proportional to the concentration of the silica suspension used. At a given nano-silica content in the pipe of 10 wt.%, the sample mass reaches 2.0 wt.% mass gain after 28 days (Fig. 8a). A comparison between nano-silica and silica fume shows the effect of particle size on the injection: doubling the concentration of nano-silica results in a mass increase of ca. +1% of the original value, whereas doubling the silica fume content results in an increase of ca. +0.1% (Fig. 8b). This is probably due to the low particle size range of

nano-silica (5–20 nm), able to penetrate into smaller pores. Open porosity measurements show that an increase in nano-silica content in the solution produces a significant decrease in porosity of ca. 30%, from the initial value (sample OPC, f= 0:30) to the highest concentration at 20 wt.%. (sample S20-14 f= 0:21), as shown in Figure 8b. Injection of silica-fume, does not produce a significant porosity reduction [28].

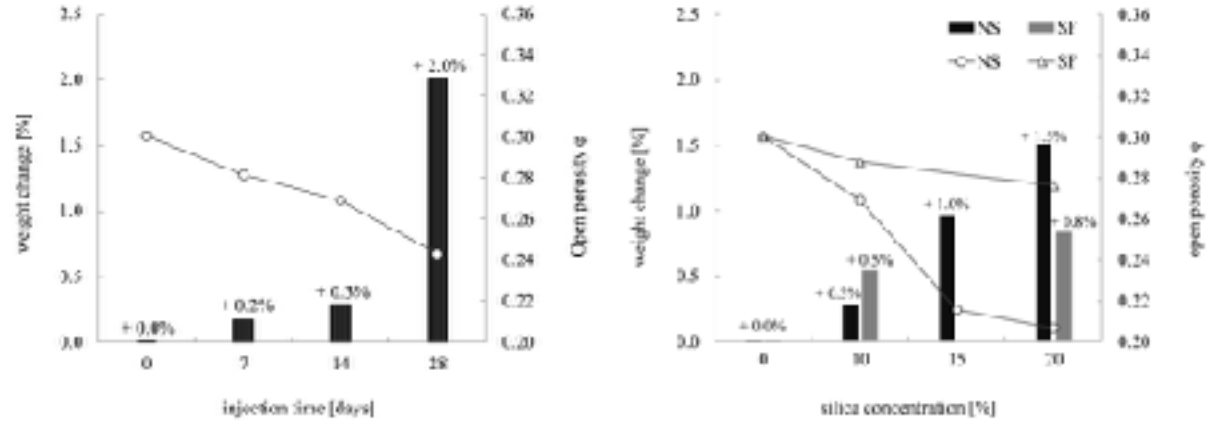

(a) (b)

Figure 8a. Influence of injection time on mass increase and open porosity using a 10 wt.% nano-silica suspension. Figure 8b: Influence of silica suspension concentration on mass increase and open porosity after injection for 14 days. [Bars represent mass change and open circles and triangles represent porosity values].

Fig. 9 shows the reduction of portlandite (CH) as it reacts with nanosilica to form additional C-S-H, which was quantified by XRD analysis.

This reduction of portlandite by c. 40% from the initial portlandite content is higher in comparison with the values found in literature [26, 29], due to a longer treatment time and higher applied pressure. There is no evidence of increased portlandite reduction when the nano-silica suspension concentration is increased beyond 15 wt.% in the injecting solution. The total increase of C-S-H formed, c. 20% with respect to the original value, is over-estimated by TGA, due to the presence of other minor compounds in the same temperature range (80–150 ^{o}C). Accurate estimation is given by semi-quantitative analyses of XRD patterns. Fig. 9 suggests that the ideal injection period is 14 days, producing a portlandite reduction of c. 40%. TG analysis of nano-silica and silica fume for 14 days injection time show that both materials offer a comparable portlandite reduction at the highest concentration (20 wt.%).

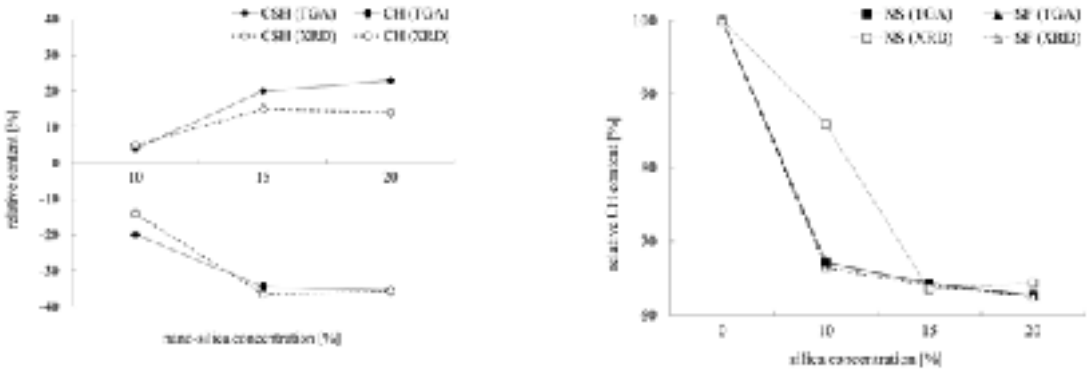

(a) (b)

Figure 9 Comparison between TGA results and semi-quantitative analysis of XRD data. (a) Effect of nano-silica solution wt. % on relative increase of C-S-H and decrease of CH compared to the OPC control sample for 14 days of injection. (b) Effect of silica particle-size and concentration on the CH relative content after 14 days of injection.

REAL-TIME MANAGEMENT OF AUTONOMOUS SYSTEMS FOR DECOMMISSIONING

Research on real-time management of autonomous systems for decommissioning in the DISTINCTIVE project has focused on the use of advanced computer vision methods for 3D characterization of buildings, scenes or objects, during nuclear decommissioning, especially decommissioning operations which rely on robotic interventions. Before any decommissioning operations can begin, the facility or materials being decommissioned must be “characterized”, which includes 3D mapping and modeling, as well as identifying types and severities of nuclear, chemical, thermal or other hazards. In particular, it is very important to identify the kinds of materials which are present in a scene. 3D reconstruction may be needed for concrete-shielded rooms or "caves", containing legacy plant (e.g. pipes and vessels) which will need to be cut and dismantled by a robot and then packed into safe storage containers. Many such caves are many decades old, and their content uncertain. They must be cut open and sorted through by robots. Real-time 3D modeling of these heaps of assorted objects is necessary to enable robotic grasping and manipulation. Furthermore, identification of types of materials is also critically important, so that low-level waste can be placed into relatively cheap containers and waste processing routes, while more dangerous waste can be accurately identified and placed into much more expensive containers for longer-term storage.

Research under the structural integrity theme has addressed the problem of developing new computer vision methods for real-time, semantic, 3D reconstruction of nuclear waste scenes.
This involves real-time 3D reconstruction of a scene, but also involves simultaneously recognizing different types of materials or objects that are present in the scene, and using these material/object categories to “semantically” label all parts of the 3D scene model.

Figure 10. Samples of 2D-3D nuclear material database.

The 2D-3D Nuclear Dataset and Virtual Camera System

After talking directly with nuclear decommissioning experts and obtaining the pictures of real nuclear wastes, a 2D-3D nuclear waste database was built. This dataset includes the metal, can, wood, bottle, brick, chain, pipe, sponge, glove, fabric and etc., as shown in Figure 10. It contains a large number of RGB images, depth images and 3D point cloud models. The 3D model of the nuclear object can be obtained from RGBD SLAM. Meanwhile the RGB and depth images of the key frame can be obtained. After getting the 3D object model, millions of labelled RGB-D images can be obtained from different viewpoints using our virtual camera system for deep learning training. Ground-truth 6DOF camera trajectories can also be provided by the virtual camera system as a benchmark for 3D reconstruction.

Research under this project addresses the problem of RGBD object recognition in real-world applications, where large amounts of annotated training data are typically unavailable. To overcome this problem, a novel, weakly-supervised learning architecture (DCNNGPC) has been developed which combines parametric models (a pair of Deep Convolutional Neural Networks (DCNN) for RGB and D modalities) with non-parametric models (Gaussian Process Classification). The system is initially trained using a small amount of labelled data, and then automatically propagates labels to large-scale unlabelled data. 3D-based objectness detection is first run on RGBD videos to acquire many unlabeled object proposals, and then DCNN-GPC is employed to label them. The resulting multi-modal DCNN can be trained end-to-end using only a small amount of human annotation. Finally, 3D-based objectness detection and multimodal DCNN has been integrated into a real-time detection and recognition pipeline. In this approach, bounding box annotations are not required and boundary-aware detection is achieved. A novel method to pre-train a DCNN for the depth modality has been developed, by training on virtual depth images projected from CAD models. The multi-modal DCNN is pretrained on public 3D datasets, achieving performance comparable to state-of-the-art methods on the Washington RGBS Dataset.
The network is then fine tuned by further training on a small amount of annotated data from the dataset of industrial nuclear waste objects (nuclear waste simulants) described above (Fig. 10). Our weakly supervised approach has been shown to be highly effective in solving novel RGBD object recognition applications which lack human annotations.

The Pipeline Of The Work
The proposed work pipeline (Fig. 11 and Fig. 12) has three steps: (1) a real-time 3D-based object detection approach to generate high-quality objectness proposals in RGBD video stream; (2) DCNN-GPC to propagate small-scale labeled data to moderate-scale in order to train the multi-modal DCNN end-to-end; (3) real-time detection is integrated with the recognition system.

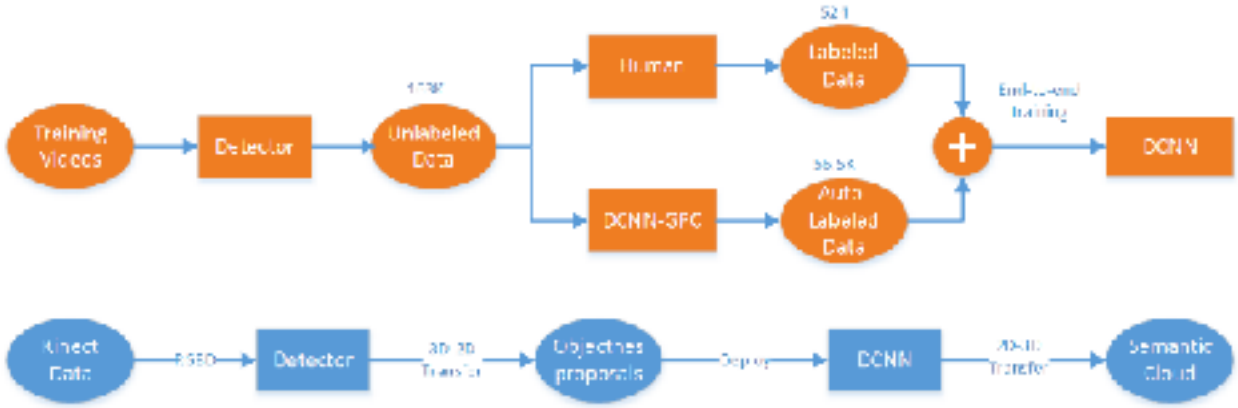

Figure 11 Flow chart of our proposed weakly-supervised DCNN method. Training is shown in orange and deployment in blue.

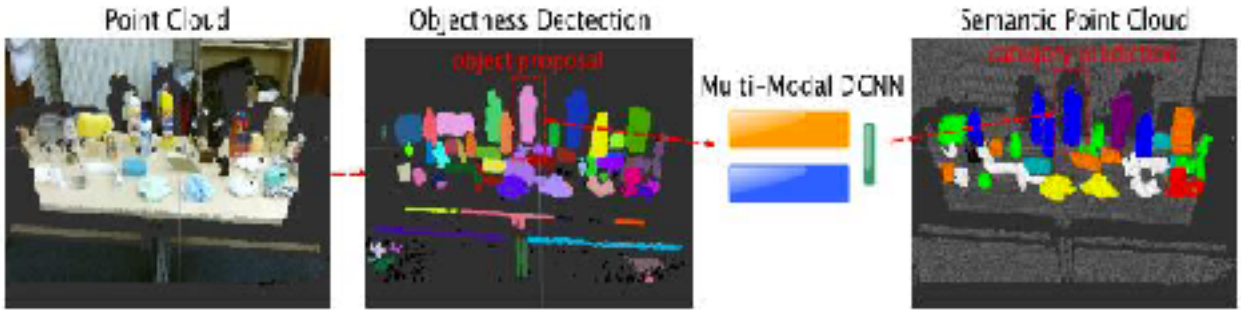

Figure 12 RGBD point cloud (left) yields objectness proposals (middle). For each such proposal, the multi-modal DCNN performs category recognition. The pixel-wise recognition result is projected to obtain a 3D semantic cloud.

The main contributions in the area of real-time management of autonomous systems for decommissioning are: 1) Previous RGBD object recognition methods have predominantly been fully-supervised, making them unsuitable for rapid deployment in new applications. In contrast, this research uses a weakly supervised method, based on Gaussian Process Classification (GPC) combined with DCNN deep learning. Unlike previous work, the method does not require bounding box object annotation, and uses very little manually-labeled data (0.3%). 2) The approach presented here learns directly from raw depth images, in contrast to previous work which relies on extracting low-level features or color-mapping. A new method is adopted to pre-train the depth DCNN by using many automatically generated synthetic depth images. 3) A new industrial dataset has been constructed, comprising RGBD videos of realistic nuclear waste-like objects. The real-time detection and recognition system has been implemented and significantly outperforms a fully supervised method i.e. R-CNN on this real-world data.

CONCLUSIONS

This paper presents highlights from research under the Structural Integrity Theme of the UK DISTINCTIVE project. We present research highlights from three specific areas. Key findings are:

(1) In-situ barriers for groundwater protection;

- An analytical model has been developed for gelling of the grout in natural environments that accounts for changes in pH, electrolyte concentration, cation valence, cation molar mass, silica particle size and silica concentration.
- A numerical model has been developed and validated that can simulated grout penetration
- Mechanical tests show that colloidal-silica grouted sand is a feasible intervention to prevent soil consolidation and to increase soil stability, whilst also proving a low permeability barrier.
- Preliminary tests on grouted soil desorption showed that colloidal-silica grouting inhibits Sr and Cs desorption from contaminated soil.
- Low-pressure (20 kPa) silica injection has effectively impregnated cement samples. After 14 days of injection with a nano-silica suspension of 20 wt.% concentration we observed a total reduction of 30% in porosity from the starting value, suggesting this is a potential consolidant for friable or cracked concrete.

(2) Consolidation in cement and concrete;

- Nano-silica injection is more efficient than silica fume, due to its smaller particle size allowing it to penetrate further into the pore structure and react to produce more C-S-H.
- Some of the silica injected has reacted with the calcium hydroxide naturally present in hydrated cement, forming additional binding phases such as C-S-H (and C-A-S-H, calcium-aluminium-silicate hydrate). Unreacted silica however has been absorbed and acts as a filler agent reducing porosity.

(3) Real-time management of autonomous systems for decommissioning;

- A weakly supervised method has been developed, based on Gaussian Process Classification (GPC) combined with DCNN deep learning. Unlike previous work, the method does not require bounding box object annotation, and uses very little manually-labeled data (0.3%).

- The approach learns directly from raw depth images and new method is adopted to pre-train the depth DCNN by using many automatically generated synthetic depth images.
- A new industrial dataset has been constructed, comprising RGBD videos of realistic nuclear waste-like objects. The real-time detection and recognition system has been implemented using this database and significantly outperforms a fully supervised method i.e. R-CNN on real-world data.

ACKNOWLEDGEMENTS

The authors gratefully acknowledge the financial support of the Research Councils' UK Energy Programme under grant EP/L014041/1, "Decommissioning, Immobilisation and Storage Solutions for Nuclear Waste Inventories (DISTINCTIVE)", and for the additional support provided by our key industry partners, NDA, NNL and Sellafield Ltd. We also acknowledge the support from all members of our International Advisory Group and all industrial project supervisors.

REFERENCES

1. Jurinak, J. and L. Summers, *Oilfield applications of colloidal silica gel.* SPE production engineering, 1991. **6**(04): p. 406-412.
2. Gallagher, P.M., *Passive Site Remediation for Mitigation of Liquefaction Risk*, in *Civil and Environmental Engineering*. 2000, Virginia Polytechnic Institute and State University.
3. Noll, M.R., C.L. Bartlett, and T.M. Dochat. *In situ permeability reduction and chemical fixation using colloidal silica*. in *Proceedings of the Sixth National Outdoor Action Conference*. 1992.
4. Yossapol, N. and J. Meegoda, *Remediation of Heavy Metal Contaminated Soil with Colloidal Silica.* Hazardous and industrial wastes, 2000. **32**: p. 787-798.
5. Persoff, P., et al., *Injectable barriers for waste isolation*. 1995, Lawrence Berkeley Lab., CA (United States).
6. Moridis, G., et al., *A field test of permeation grouting in heterogeneous soils using a new generation of barrier liquids.* Committed To Results: Barriers for Long-Term Isolation. ER, 1995. **95**.
7. Moridis, G., et al. *A field test of a waste containment technology using a new generation of injectable barrier liquids*. 1996.
8. Moridis, G., A. James, and C. Oldenburg, *Development of a design package for a viscous barrier at the Savannah River site*. 1996, Lawrence Berkeley National Lab., CA (United States). Funding organisation: USDOE Office of Environmental Restoration and Waste Management, Washington, DC (United States).
9. Moridis, G.J., S. Finsterle, and J. Heiser, *Evaluation of alternative designs for an injectable barrier at the Brookhaven National Laboratory Site, Long Island, New York.* Water Resources Research, 1999. **35**(10): p. 2937-2953.
10. Hakem, N., et al. *Sorption of cesium and strontium on Savannah River soils impregnated with colloidal silica*. in *International Containment Technology Conference*. 1997. Petersburg:[sn].
11. Manchester, K., et al. *Grout selection and characterization in support of the colloidal silica barrier deployment at Brookhaven National Laboratory*. in *Proc. 2001 International Contain. and Remed. Technol. Conf. and Exhib., 10-13 June, 2001. Orlando, FL*. 2001.
12. Persoff, P., et al., *Effect of dilution and contaminants on sand grouted with colloidal silica.* Journal of geotechnical and geoenvironmental engineering, 1999. **125**(6): p. 461-469.
13. Axelsson, M., *Mechanical tests on a new non-cementitious grout, silica sol: A laboratory study of the material characteristics.* Tunnelling and underground space technology, 2006. **21**(5): p. 554-560.
14. Butrón, C., M. Axelsson, and G. Gustafson, *Silica sol for rock grouting: Laboratory testing of strength, fracture behaviour and hydraulic conductivity.* Tunnelling and underground space technology, 2009. **24**(6): p. 603-607.

15. Funehag, J. and Å. Fransson, *Sealing narrow fractures with a Newtonian fluid: Model prediction for grouting verified by field study.* Tunnelling and underground space technology, 2006. **21**(5): p. 492-498.
16. Funehag, J. and G. Gustafson, *Design of grouting with silica sol in hard rock–New design criteria tested in the field, Part II.* Tunnelling and underground space technology, 2008. **23**(1): p. 9-17.
17. Butrón, C., et al., *Drip sealing of tunnels in hard rock: A new concept for the design and evaluation of permeation grouting.* Tunnelling and underground space technology, 2010. **25**(2): p. 114-121.
18. Bahadur, A., K. Holter, and A. Pengelly. *Cost-effective pre-injection with rapid hardening microcement and colloidal silica for water ingress reduction and stabilisation of adverse conditions in a headrace tunnel*. in *Underground Space–The 4th Dimension of Metropolises, Three Volume Set+ CD-ROM: Proceedings of the World Tunnel Congress 2007 and 33rd ITA/ AITES Annual General Assembly, Prague, May 2007*. 2007. CRC Press.
19. Pedrotti, M., et al., *An analytical model for the control of silica grout penetration in natural groundwater systems.* Tunnelling and Underground Space Technology, 2017.
20. Wong, C., et al., *A study on the mechanical interaction between soil and colloidal silica gel for ground improvement.* Acta Geotechnica, 2017(under review).
21. Pellenq, R.-M., N. Lequeux, and H. Van Damme, *Engineering the bonding scheme in C–S–H: The iono-covalent framework.* Cement and Concrete Research, 2008. **38**(2): p. 159-174.
22. Chen, J.J., et al., *Solubility and structure of calcium silicate hydrate.* Cement and Concrete Research, 2004. **34**(9): p. 1499-1519.
23. Stumm, A., et al., *Incorporation of zinc into calcium silicate hydrates, Part I: formation of CSH (I) with C/S= 2/3 and its isochemical counterpart gyrolite.* Cement and Concrete Research, 2005. **35**(9): p. 1665-1675.
24. Wieland, E., et al., *Strontium uptake by cementitious materials.* Environmental science & technology, 2007. **42**(2): p. 403-409.
25. Sanchez, F. and K. Sobolev, *Nanotechnology in concrete–a review.* Construction and building materials, 2010. **24**(11): p. 2060-2071.
26. Sánchez, M., M. Alonso, and R. González, *Preliminary attempt of hardened mortar sealing by colloidal nanosilica migration.* Construction and Building Materials, 2014. **66**: p. 306-312.
27. Maddalena, R. and A. Hamilton, *Low-pressure silica injection for porosity reduction in cementitious materials*. Construction and Building Materials, 2017. **134**: p. 610-616.
28. Qing, Y., et al., *Influence of nano-SiO_2 addition on properties of hardened cement paste as compared with silica fume.* Construction and building materials, 2007. **21**(3): p. 539-545.
29. Cardenas, H.E. and L.J. Struble, *Electrokinetic nanoparticle treatment of hardened cement paste for reduction of permeability.* Journal of materials in civil engineering, 2006. **18**(4): p. 554-560.